Characterization and tissue-specific expression of two lepidopteran farnesyl diphosphate synthase homologs: Implications for the biosynthesis of ethyl-substituted juvenile hormones

ARTICLE *in* PROTEINS STRUCTURE FUNCTION AND BIOINFORMATICS · NOVEMBER 2006

Impact Factor: 2.63 · DOI: 10.1002/prot.21057 · Source: PubMed

12 AUTHORS, INCLUDING:

Michel Cusson
Natural Resources Canada
94 PUBLICATIONS **1,644** CITATIONS
SEE PROFILE

Sophie Vandermoten
University of Liège
15 PUBLICATIONS **278** CITATIONS
SEE PROFILE

Frédéric Francis
University of Liège
240 PUBLICATIONS **2,047** CITATIONS
SEE PROFILE

Eric Haubruge
University of Liège
407 PUBLICATIONS **4,580** CITATIONS
SEE PROFILE

PROTEINS: Structure, Function, and Bioinformatics 65:742–758 (2006)

Characterization and Tissue-Specific Expression of Two Lepidopteran Farnesyl Diphosphate Synthase Homologs: Implications for the Biosynthesis of Ethyl-Substituted Juvenile Hormones

Michel Cusson,[1,2]* Catherine Béliveau,[1] Stephanie E. Sen,[3] Sophie Vandermoten,[4] Robert G. Rutledge,[1] Don Stewart,[1] Frédéric Francis,[4] Éric Haubruge,[4] Peter Rehse,[5] David J. Huggins,[6] Ashley P.G. Dowling,[7] and Guy H. Grant[8]

[1]*Natural Resources Canada, Canadian Forest Service, Laurentian Forestry Centre, Québec City, Québec G1V 4C7, Canada*
[2]*Département de biochimie et de microbiologie, Université Laval, Québec City, Québec G1K 7P4, Canada*
[3]*Department of Chemistry, Indiana University-Purdue University at Indianapolis (IUPUI), Indianapolis, Indiana 46202*
[4]*Unité d'entomologie fonctionnelle et évolutive, Faculté universitaire des sciences agronomiques de Gembloux, Gembloux, B-5030, Belgium*
[5]*RIKEN Harima Institute, Mikzuki-cho, Sayo-gun, Hyogo 679-5148, Japan*
[6]*Department of Chemistry, Physical and Theoretical Chemistry Laboratory, University of Oxford, Oxford OX1 3QZ, United Kingdom*
[7]*Department of Entomology, University of Kentucky, Lexington, Kentucky 40546-0091*
[8]*Unilever Centre for Molecular Informatics, University of Cambridge, The University Chemical Laboratory, Cambridge CB2 1EW, United Kingdom*

ABSTRACT **The sesquiterpenoid juvenile hormone (JH) regulates insect development and reproduction. Most insects produce only one chemical form of JH, but the Lepidoptera produce four derivatives featuring ethyl branches. The biogenesis of these JHs requires the synthesis of ethyl-substituted farnesyl diphosphate (FPP) by FPP synthase (FPPS). To determine if there exist more than one lepidopteran FPPS, and whether one FPPS homolog is better adapted for binding the bulkier ethyl-branched substrates/products, we cloned three lepidopteran FPPS cDNAs, two from *Choristoneura fumiferana* and one from *Pseudaletia unipuncta*. Amino acid sequence comparisons among these and other eukaryotic FPPSs led to the recognition of two lepidopteran FPPS types. Type-I FPPSs display unique active site substitutions, including several in and near the first aspartate-rich motif, whereas type-II proteins have a more "conventional" catalytic cavity. In a yeast assay, a *Drosophila* FPPS clone provided full complementation of an FPPS mutation, but lepidopteran FPPS clones of either type yielded only partial complementation, suggesting unusual catalytic features and/or requirements of these enzymes. Although a structural analysis of lepidopteran FPPS active sites suggested that type-I enzymes are better suited than type-II for generating ethyl-substituted products, a quantitative real-time PCR assessment of their relative abundance in insect tissues indicated that type-I expression is ubiquitous whereas that of type-II is essentially confined to the JH-producing glands, where its transcripts are ~20 times more abundant than those of type-I. These results suggest that type-II FPPS plays a leading role in lepidopteran JH biosynthesis in spite of its apparently more conventional catalytic cavity. Proteins 2006;65:742–758.**

Key words: JH homologs; mevalonate pathway; FPPS; gene structure; FARM; homology modeling; docking; yeast complementation assay; quantitative real-time PCR

INTRODUCTION

The sesquiterpenoid juvenile hormone (JH) is a key regulator of insect development and reproduction. In immature insects, high titers of this hormone prevent the precocious onset of metamorphosis whereas in adults, it promotes ovarian maturation and regulates various other aspects of reproduction. Six different chemical forms of JH have so far been identified in the class Insecta, with the 10-11-epoxy methyl-ester derivative of farnesyl diphosphate (FPP), JH III (or C16-JH), being the only JH found in most species. The Lepidoptera (i.e., caterpillars, moths, butterflies), however, display an apparently singu-

Grant sponsor: Canadian Biotechnology Strategy Fund.

David J. Huggins's current address is Computer Science and Artificial Intelligence Laboratory, Biological Engineering Division, Massachusetts Institute of Technology, Cambridge, MA.

*Correspondence to: Michel Cusson, Laurentian Forestry Centre, PO Box 10380, Stn. Sainte-Foy, Québec, QC G1V 4C7, Canada. E-mail: michel.cusson@nrcan.gc.ca

Received 6 May 2005; Revised 7 April 2006; Accepted 19 April 2006

Published online 13 September 2006 in Wiley InterScience (www.interscience.wiley.com). DOI: 10.1002/prot.21057

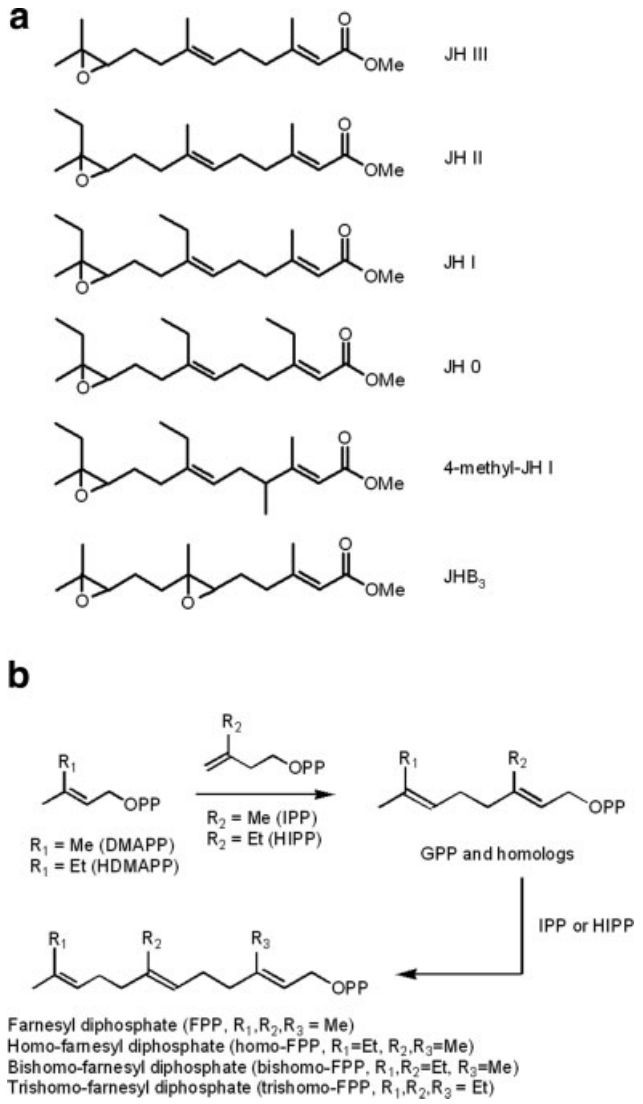

Fig. 1. **(a)** Structures of the six known juvenile hormones (JHs). JH 0, JH I, JH II, and 4-methyl-JH I have so far been found only in the Lepidoptera. JHB_3 is a bisepoxide form of JH III found in the higher Diptera.[1] **(b)** Reactions catalyzed by lepidopteran FPPS.

lar ability to produce ethyl-branched JHs, four of which have been reported since 1967: JH II (C17-JH), JH I (C18-JH), JH 0 (C19-JH), and 4-CH_3-JH I (Me-C19-JH) [Fig. 1(a)].

Ever since their discovery, JH molecules have intrigued insect physiologists and biochemists alike since natural sesquiterpenes rarely contain ethyl branches.[2] FPP is formed by FPP synthase (FPPS; EC 2.5.1.10), a prenyltransferase that catalyzes the head-to-tail coupling of three isoprene (C5) units, namely isopentenyl diphosphate (IPP) and its allylic isomer, dimethylallyl diphosphate (DMAPP). The latter serves as the chain initiator, with the first coupling leading to the formation of the C10 intermediate, geranyl diphosphate [GPP; Fig. 1(b)]. In a landmark study, Schooley et al.[3] provided clear evidence that the ethyl branches of lepidopteran JHs do not arise from the selective methylation of the JH carbon skeleton at a step subsequent to the formation of FPP. Rather, these branches are introduced very early in JH biosynthesis, with propionyl-CoA substituting for acetyl-CoA in a condensation reaction catalyzed by HMG-CoA synthase. The homo-HMG-CoA thus produced is converted to homo-IPP which, along with its isomers homo-DMAPP and (*E*)-3-methyl-3-pentenyl diphosphate, may act as alternative substrate for FPPS. Independent studies[4,5] indicated that an FPPS purified from pig liver could, under extended incubation, use ethyl-substituted isoprene substrates (C6) to produce the farnesyl-related precursors of the lepidopteran JHs, although isomeric skeletons of the natural hormones were also formed.

JH is produced by a pair of minute endocrine glands known as the corpora allata (CA). Within the lepidopteran CA, propionyl-CoA is derived primarily from the metabolism of the branched-chain amino acids (BCAA) isoleucine and valine.[6] BCAA transaminase catalyzes the first step of this conversion.[7] Interestingly, the CA of insects producing only JH III are unable to convert BCAAs into propionate[8] because of the absence of an active BCAA transaminase.[7] Hence, this enzyme is critical for the accumulation of propionate within the lepidopteran CA and constitutes a unique feature of the lepidopteran JH biosynthetic machinery. The activity of this enzyme in the CA of the armyworm moth, *Pseudaletia* (syn. *Mythimna*) unipuncta, has been shown to correlate with the animal's requirements for propionyl-CoA in JH and JH acid (JHA) biosynthesis. However, variations in the activity of this enzyme cannot alone explain the change in the proportions of the various JH structures observed in the course of an insect's life.[9] Thus, the substrate specificity and activity of other enzymes in the JH biosynthetic pathway must be invoked to fully explain JH homology.

Early studies designed to assess the substrate specificity of enzymes in the JH biosynthetic pathway (from the point of biogenesis of HMG-CoA) suggested rather loose substrate specificity,[2] although several workers have argued that some differences in specificity must exist between JH III-producing insects and the Lepidoptera.[10,11] In this context, FPPS is seen as the JH biosynthetic enzyme most likely to show some level of substrate and product selectivity because its active site must be able to easily take up both the C5 and C6 substrates used to generate the carbon skeleton of lepidopteran JHs.

Koyama et al.[12] succeeded in purifying two apparently different FPPSs from *Bombyx mori* whole larvae and subsequently[13] showed that "FPPS II," unlike "FPPS I," coupled bishomo-GPP to IPP more effectively than GPP when Mn^{2+} was used as cofactor. On the basis of this observation, they suggested that "FPPS II" was likely the FPPS involved in JH biosynthesis, although the high abundance of this protein in whole-body preparations suggested that its expression was not confined to the CA. Later, however, Sen et al.[14,15] developed an in vitro FPPS assay using homogenates of *Manduca sexta* larval CA, allowing measurement of FPPS activity and an assess-

ment of its specificity for ethyl-substituted substrates. A competition assay using homo-DMAPP and DMAPP revealed a 1.8:1 preference for the former substrate, independent of metal cofactor used. In addition, the C20 terpenoid geranylgeranyl diphosphate completely inhibited the CA prenyl transferase, indicating that this ligand could bind tightly to the enzyme's active site in contrast to what had been reported for other FPPSs.[14] These observations suggested that the catalytic cavity of lepidopteran FPPS may be deeper than that of other FPPSs, which could represent an adaptation for handling the bulkier ethyl-branched substrates and products involved in the biosynthesis of the C17, C18, and C19 JHs.

Current knowledge about FPPS structure is based in large part on various site-directed mutagenesis studies performed on both eukaryotic and prokaryotic FPPSs and other related prenyl transferases (see Ref. 16–19), and on the work of Tarshis et al., who reported the crystal structure of unliganded chicken FPPS at a 2.6-Å resolution,[20] as well as that of the corresponding double F112A/F113S mutant bound with DMAPP, GPP, and FPP.[21] More recently, Hosfield et al.[22] determined the crystal structures of two prokaryotic FPPSs to 2.4-Å resolution; the unliganded *Staphylococcus aureus* FPPS and the *Escherichia coli* enzyme bound to both IPP and a noncleavable DMAPP analogue. Preliminary X-ray data have also been reported for *Trypanosoma brucei* FPPS,[23] and the X-ray structure of human FPPS with bound inhibitor has recently been solved (PDB:1YV5 and PDB:1YQ7; unpublished). Altogether, these studies have indicated that FPPS is a highly α-helical homodimeric protein, with 10 core helices positioned around a large central cavity, and with each subunit containing an independent catalytic cavity whose bottom wall is near the subunit interface. Up to seven conserved regions have been identified, including two that possess an aspartate-rich motif (DDx(xx)xD) and are positioned on opposite sides of the active site, where they are involved in substrate binding and catalysis. The residues at positions −4 and −5 relative to the first aspartate-rich motif ("FARM") have been shown to be involved in product chain-length specificity (C15 for FPPS versus C10, C20, or larger); therefore, the nature of these residues can affect the depth of catalytic cavity.

For the present study, we wanted to evaluate the hypothesis that the Lepidoptera, which produce FPP and homologous FPP structures, do so by the involvement of more than one FPPS, as suggested by earlier work on *B. mori.*[12,13] We were also interested in exploring the possibility that one of these proteins displays unique active site features that could confer a selectivity for ethyl-substituted substrates and products; such an enzyme would be a suitable target for the development of Lepidoptera-specific pest control products.[24] To this end, we undertook the cloning of FPPS cDNAs from two moth species belonging to phylogenetically distant families, *Choristoneura fumiferana* (Tortricidae) and *P. unipuncta* (Noctuidae), and analyzed these sequences in the context of two other lepidopteran FPPSs (*Agrotis ipsilon*[25] and *B. mori*[26]) that were reported earlier by other groups. Here, we demonstrate the existence of two distinct lepidopteran FPPS types, analyze their active site substitutions, and assess their ability to complement a yeast FPPS mutation. Last, we examine the distribution of their transcripts in various insect tissues, including the CA.

MATERIALS AND METHODS

Biological Material

Larvae of the true armyworm, *P. unipuncta*, and of the eastern spruce budworm, *C. fumiferana*, were reared on an artificial diet, and adults were provided 8% sucrose in water.[9,27] Aphids (*Aphis fabae*, *Acyrthosiphon pisum*, *Megoura viciae*, and *Myzus persicae*) were reared on bean plants as described.[28] *Drosophila melanogaster* adult flies were kindly provided by R. Tanguay, Department of Medicine, Université Laval, Canada. Cells of two spruce budworm cell lines, CF203[29] and CF124T,[30] were provided by G. Caputo (Natural Resources Canada, Sault Ste. Marie, Ontario) and grown at room temperature in Grace's modified medium as described.[31] The *Saccharomyces cerevisiae* yeast strain CC25 (Mat a, *erg*12-2, *erg*20-2, *ura*3-1, *trp*1-1)[32] was kindly provided by Dr F. Karst, Université Louis Pasteur, Strasbourg, France.

RNA and DNA Isolation

Total RNA from *P. unipuncta* adult CA, *C. fumiferana* adult brains, CF203 cells and whole body *D. melanogaster*, *A. fabae*, *A. pisum*, *M. vicia*, and *M. persicae* was extracted using TRIZOL reagent (Invitrogen) according to the manufacturer's instructions. CF124T genomic DNA was extracted as described.[31]

FPPS Partial cDNA Sequences

One microgram of total RNA (*P. unipuncta*, *C. fumiferana*, *A. pisum*, *M. vicia*, and *M. persicae*) was reverse transcribed using 0.2 μg of an oligo$(dT)_{12–18}$ primer and 200 U SuperScript II RNase H^- reverse transcriptase (Invitrogen). The reaction was carried out in 1× PCR buffer (10 m*M* Tris-HCl, 1.5 m*M* $MgCl_2$, 50 m*M* KCl pH 8.3) with 0.5 m*M* of each dNTP and 18 U of RNAguard ribonuclease inhibitor (Amersham Biosciences) at 42°C for 1 h. Highly conserved regions among known FPPS proteins were identified from the sequence alignment of selected representatives (*A. ipsilon* AJ009962, *D. melanogaster* AF132554, *S. cerevisiae* J05091, *Neurospora crassa* X96944, *Arabidopsis thaliana* U80605, *Rattus norvegicus* M17300, and *Homo sapiens* J05262). These regions were used to design two degenerate forward primers, namely P1 and P3, as well as two reverse primers, P2 and P4 (Table I), corresponding respectively to the segments YNVPNGKKNRG, MRRGAPCW, GKNGTDIQD, and FFQIQDDFLD of the *A. ipsilon* FPPS (*Ai*FPPS) amino acid sequence. One sixth of the reverse transcription reaction was used for PCR amplification with 1 μ*M* of P1 and P2 as primers, and 0.2 m*M* of each dNTP in 1× PCR buffer. A "hot start" PCR was achieved by addition of 2.5 U of *Taq* 2000 DNA polymerase (Stratagene) after a

TABLE I. Designations, Orientations, Oligonucleotide Sequences, and Positions Within the cDNA Sequences of the Primers Used for PCR Cloning of Insect FPPSs

Specificity	Name	Orientation	5′ → 3′ primer sequence[1]	Position
Highly conserved FPPS regions	P1	Forward	TAYAAYRYIVBIVRIGGIAARHWIAAYMGNGG	—
	P2	Reverse	RTCYTGDATRTCIGTICCIWYYTTNCC	—
	P3	Forward	AYIMGIMGIGGIVMIMYITGYTGG	—
	P4	Reverse	TCIARRWARTCRTCYTGIAYYTGRAARWA	—
cDNA (3′RACE)	AP	Reverse[2]	GGCCACGCGTCGACTAGTAC(T)$_{17}$[3]	—
	AUAP	Reverse[2]	GGCCACGCGTCGACTAGTAC[3]	—
P. unipuncta FPPS	SP-1	Forward	*TATCTCTAGA*CCGTCCTTGAGAC[4]	697–710
	SP-2	Reverse	GCACTTTAACAGCATCTCAT	734–716
	SP-3	Reverse	*TAGCTCTAGA*TGGCGGCTTGAATTAG[4]	650–634
	SP-4	Forward	GGGAATTC*CATATG*TTTTCAACGAAG[5]	2–27
	SP-5	Reverse	*AATTCCTCGAG*TTTAGACGCTTCGC[6]	1299–1284
C. fumiferana FPPS-1	SP-1	Forward	GCCAAGTACAAGACAGCATACCAC	935–959
	SP-4	Forward	AACG*CATATG*TTTTCAACTACGAGA[5]	122–139
	SP-5	Reverse	*TAACCTCGAG*AATTAGATGTTTCGTC[6]	1410–1395
	SP-6	Reverse	CAACATGCTTGCTGGTCTCA	454–436
	SP-7	Forward	CAGATTCCTGTCGACCCTGA	316–335
	SP-8	Reverse	GCGCTTGCTTATTGTGATGA	Intron
	SP-9	Forward	AGCCATACTACAAGAATGTGATCGAA	795–819
C. fumiferana FPPS-2	SP-1	Forward	*TAGCTCTAGA*GTCTCATGCACAC[4]	708–723
	SP-2	Reverse	CTCCATTGTAACGTCTAAGTG	757–737
	SP-3	Reverse	*TAGCTCTAGA*CGAGAACATGAGTGAG[4]	636–619
	SP-4	Forward	*ATCTGG*AT*CC*ATGAGGCTAAACAAGTG[7]	92–108
	SP-5	Reverse	*AATTCCTCGAG*CAATCAATGATTCCTCT[6]	1285–1274
	SP-6	Reverse	*TAGCTCTAGA*CGGTTATATTTTCTGGCT[4]	459–441
	SP-7	Forward	GACGACATTGTTTGCGTATGA	412–429
	SP-8	Forward	GTTCTCGTCGATATTCTACGTGC	629–649
D. melanogaster FPPS	SP-4	Forward	*GAATTCCATATG*TTTAAACTGGCCCGT[5]	83–102
	SP-5	Reverse	*AATTCCTCGAG*TAATTTAGGAGTCACG[6]	1351–1333
A. ipsilon FPPS	SP-4	Forward	GAGATTTTC*CATATG*TTCTCCACGAAG[5]	162–177
	SP-5	Reverse	*ATTCCTCGAG*TTTAAACGCTTCGC[6]	1450–1435

[1]Sequences in italics differ from the original cDNA to produce a 5′-extension or an internal restriction site.
[2]Forward orientation for the 5′RACE.
[3]Underlined, *Spe*I restriction site.
[4]Underlined, *Xba*I restriction site.
[5]Underlined, *Nde*I restriction site.
[6]Underlined, *Xho*I restriction site.
[7]Underlined, *Bam*HI restriction site.

first heating step at 94°C for 2 min. The rest of the cycling conditions were carried out as follows: 10 cycles of 94°C, 30 s; 44°C, 30 s; 72°C, 1 min; followed by 30 cycles of 94°C, 30 s, 47°C, 30 s; 72°C 1 min; and a final extension step at 72°C for 5 min. In cases where the first PCR reaction yielded no product detectable by agarose gel electrophoresis, one tenth of the first reaction was used as template for a second PCR amplification using P3 and P4 as primers, in the same buffer and with the same cycling conditions. Using the Geneclean II kit (Q-BIOgene), the bands were purified from the agarose gel and cloned in the pGEM-T Easy vector (Promega) according to the manufacturer's instructions, and sequenced.

3′ and *5′* RACE

For rapid amplification of cDNA 3′end (3′RACE), 1 μg of total RNA was reverse transcribed as before except that an Adapter Primer (AP) (Invitrogen) (Table I) containing a *Spe*I restriction site was used instead of the oligo-dT. PCR amplification was done as before using 0.25 μ*M* of FPPS specific primer-1 (SP-1), with or without a restriction site at its 5′ end, and the Abridged Universal Amplification Primer (AUAP) (Invitrogen) corresponding to the 5′ portion of the AP (Table I). The major amplification products obtained were cut out from an agarose gel after electrophoresis, purified, cloned directly in the pGEM-T Easy vector, or digested with *Xba*I and *Spe*I and cloned in the *Xba*I restriction site of the pLitmus-29 vector (New England Biolabs), prior to sequencing.

For the rapid amplification of the cDNA 5′ ends (5′RACE), 2 μg of total RNA was reverse transcribed as before with 0.1 μ*M* of FPPS specific primer-2 (SP-2, Table I) complementary to the sequence obtained by 3′RACE. After 1 h incubation at 42°C, the reaction was stopped by heating at 70°C for 15 min, followed by a treatment with 1 U of RNase H and 590 U of RNase T1 for 30 min at 37°C. The cDNA was purified with the Geneclean II kit (Q-BIOgene). A poly-A tail was added in 1× tailing buffer containing 0.2 m*M* of dATP and 15 U of

terminal deoxynucleotidyl transferase (Invitrogen), incubated at 37°C for 1 h and at 65°C for 10 min. Synthesis of the second-strand cDNA was carried out in 1× PCR buffer with 10 m*M* DTT, 0.5 m*M* of each dNTP, 0.2 μ*M* of the AP, and 200 U of SuperScript II RNase H^- reverse transcriptase (Invitrogen), at 50°C for 50 min; the double-stranded cDNA was purified using the Geneclean II kit. One fifth of double stranded cDNA produced was used for PCR amplification, using 0.25 μ*M* of the AUAP and SP2 in 1× PCR buffer containing 0.4 m*M* of each dNTP, an additional 1 m*M* $MgCl_2$ (giving a final concentration at 2.5 m*M*) and 5% DMSO. The cycling conditions were the same as those described for amplification with degenerate primers except that the elongation step at 72°C was extended to 2 min. One tenth of the first amplification reaction was used as template for a second PCR amplification with the AUAP and a nested FPPS specific primer-3 (SP-3, Table I) containing an *Xba*I restriction site at its 5′ end. The reaction was carried out in the same buffer and with the same cycling conditions as before. Following electrophoresis, the amplicon that stood out from the smear was cut from the agarose gel and purified, digested with *Spe*I and *Xba*I, cloned in the *Xba*I restriction site of pLitmus-29 (New England Biolabs) and submitted to sequencing.

Cloning the FPPS cDNA in Expression Vectors, Yeast Transformation, and Complementation Assays

Two micrograms of total RNA from *P. unipuncta*, *C. fumiferana*, and *D. melanogaster* was reverse transcribed as described above for the 3′RACE. One sixth of the reverse-transcription reaction for each of these three species, or 10 ng of the *Ai*FPPS cDNA (kindly provided by Franck Couillaud, Université de Bordeaux I, France), was used for PCR amplification with 2.5 U of *Pfx* DNA polymerase (Invitrogen) in 1× *Pfx* buffer, 0.3 m*M* of each dNTP, 1 m*M* $MgSO_4$, and 0.3 μ*M* of each FPPS specific primer pair (forward SP-4 and reverse SP-5; Table I). Primer design included an *Nde*I or a *Bam*HI site 5′ extension immediately upstream of the initiation codon, and a 5′ extension creating a *Xho*I restriction site after the stop codon. The cycling conditions were as follows: a first heating step at 94°C for 2 min; then 5 cycles of 94°C, 15 s; 44°C, 30 s; 68°C, 1 min 30 s; followed by 30 cycles of 94°C, 15 s; 47°C, 30 s; 68°C, 1 min 30 s, and a final extension step at 68°C for 5 min. The amplicons were cloned into either of the pET28a(+) (Novagen) or pGEM-T-Easy (Promega) vectors, and sequenced.

To express the FPPS cDNA in yeast under the control of the strong phosphoglycerate kinase promoter, the *Nde*I-*Xho*I fragment (*A. ipsilon*, *D. melanogaster*, *P. unipuncta*) and the *Bam*HI-*Xho*I fragment (*C. fumiferana* FPPS-2) from the pET28 clones, and the *Nde*I-*Eco*RI fragment (*C. fumiferana* FPPS-1) from pGEM-T-Easy vector, were ligated in the *Not*I restriction site of the pFL61 vector (ATCC77215).[33] To form blunt ends, all 5′ overhangs were filled-in using Klenow in the presence of dNTP prior to ligation. Orientation of the resulting clones was ascertained by restriction analysis. The yeast strain CC25 was transformed using the ECM 830 electroporator (BTX). The cells were grown at 28°C to a density of 1×10^7 cells/mL in YPD medium (Difco) supplemented with 4 μg/mL ergosterol (Sigma) from a stock solution (4 mg/mL) in a mixture of Tergitol NP40 (Sigma)/ethanol (1:1 v/v), pretreated for 30 min at 28°C after adding 25 m*M* DTT to the culture medium, centrifuged and washed twice in electropermeabilization buffer (10 m*M* Tris-HCl, pH 7.5, 270 m*M* sucrose and 1 m*M* $MgCl_2$), as described.[34] The cells were finally resuspended in electropermeabilization buffer at a concentration of 5×10^7 cells per assay, in the presence of 1 μg plasmid DNA. After electroporation (LV mode, 270 V, 1 pulse of 11 ms in 1 mm gap disposable cuvette), the cells were transferred in 1 mL of YPD-ergosterol (4 μg/mL) and incubated for 1 h at 28°C before plating them on minimal medium [0.67% (w/v) yeast nitrogen base without amino acids, 2% (w/v) dextrose, 50 μg/mL tryptophan, and 80 μg/mL ergosterol]. The complementation assay was initiated by inoculating 25 mL of liquid minimal medium with enough inoculum from a preculture to achieve an OD_{600} of 0.055 ± 0.005, followed by incubation at 28°C with shaking. To monitor the growth, the OD_{600} was measured at different intervals over a period of 77 h.

Phylogenetic Analysis

Amino acid and nucleotide sequences reported here and those of selected eukaryotic and prokaryotic FPPSs were aligned using ClustalX[35] and default settings. The results of separate nucleotide alignment with subsequent conversion to amino acids and direct amino acid alignment were equivocal. Only those FPPSs for which a full sequence was available were included in the analysis, except for *B. mori* FPPS-2 (*Bm*FPPS-2), whose N-terminal sequence is incomplete (see Fig. 4). The resulting amino acid alignment was trimmed after the stop codon and analyzed heuristically in PAUP*[36] using parsimony optimality criterion with informative characters treated as unordered and unweighted. The analysis consisted of 1000 random addition replicates with tree-bisection-reconnection branch swapping retaining all most parsimonious trees found. Support for nodes was calculated using 10,000 bootstrap pseudoreplicates, each consisting of heuristic searches including 20 random addition replicates and tree-bisection-reconnection branch swapping. A majority rule bootstrap consensus was retained, collapsing all branches with less than 50% bootstrap support.

C. fumiferana FPPS-1 and FPPS-2 Genomic Sequences

A series of specific primer combinations were used to amplify the *C. fumiferana* FPPS-1 (SP-4/SP-6, SP-7/SP-8, SP-9/SP-5) and FPPS-2 (SP-4/SP-6, SP-7/SP-2, SP-8/SP-5) genomic fragments (see Table I for primer sequences). The amplification reactions were carried out using 100 ng of CF124T genomic DNA, 0.25 μ*M* of a given forward and

reverse specific primer combination, and 1 U of Platinum Taq DNA polymerase High Fidelity (Invitrogen) in 1× High Fidelity PCR Buffer, supplemented with 2 m*M* $MgSO_4$. The cycling conditions were as follows: a first heating step at 94°C for 90 s; then 30 cycles of 94°C, 45 s; 52°C, 45 s; 68°C, 6 min; and a final extension step at 68°C, 10 min. Before gel purification of the amplicons, a 15-min posttreatment with 1 U of Taq DNA polymerase at 72°C was needed for TA cloning in the pGEM-T-Easy vector. For the longer cloned genomic fragments, subcloning of shorter, overlapping fragments was necessary to obtain the complete sequence.

For comparative purposes, the genomic sequences of two *Bm*FPPSs were gleaned from public data bases searched through the NCBI Web site (http://www.ncbi.nlm.nih.gov/BLAST/Genome/Insects.html), whereas the sequence of *D. melanogaster* FPPS was obtained directly at the Flybase Web site (http://flybase.bio.indiana.edu/).

Homology Modeling of *P. unipuncta* FPPS

P. unipuncta FPPS was modeled using an avian FPPS mutant complexed with FPP (PDB code 1UBX) as template.[21] The identity between the two structures was 44%. The biological dimer structure was generated by applying crystallographic transformation described in the PDB entry to both the protein and the substrate. The initial modeling was performed with InsightII (Accelyrs), with energy minimization performed by CHARMM[37] within Quanta (Accelyrs). Residue 20 of the avian structure corresponds to residue 81 of the moth model and hence the first 80 residues of the latter protein were not modeled. PROCHECK[38] was used for stereochemical analysis. Residues demonstrating large deviations in chi angles were remodeled using the rotation library in Quanta with secondary adjustments of neighboring residues if clashes occurred. The R.M.S. deviation between avian structure and moth model was 0.611 Å. Molecular images were generated using Swiss-PdbViewer (DeepView).[39]

Docking

The FPPS structures used for the docking simulations were those of the moth model described above and of the avian structure 1UBX. For the latter, however, the two monomers were first combined to form a homodimer, and Ala112 and Ser113 were replaced with Phe residues; the resulting structure was energy-minimized using CHARMM.[40] Four putative ligands were created using InsightII: FPP, homo-FPP, bishomo-FPP, and trishomo-FPP. All atom positions were based on the coordinates of the FPP molecule from the 1UBX complex. The atom-centered partial charges were assigned by CHARMM.[40] The four ligands were then docked to both FPPS structures using the docking algorithm *Eve* (Huggins D, Grant GH. J Med Chem, Submitted). *Eve* is a grid-based docking algorithm that uses a multiscale approach to find best orientation before optimization begins. The ligand is represented initially as one feature point and the lowest energy points used to create the second generation in which the ligand is represented as two points. The lowest energy points then become the third generation in which the ligand is represented as three points. Once the best orientations have been calculated, docking is performed on the whole molecule (ligand). The remaining solutions become the first generation for a genetic algorithm to optimize the three-dimensional structure and calculate the binding energy.

Assessment of Tissue-Specific Transcription of FPPS-1 and FPPS-2 by q-RT-PCR

Silkworm larvae were obtained from LiveFood.ca (Montreal, Canada) as newly molted fourth instars (L4) and reared on an artificial diet containing 30% dehydrated mulberry leaves. Some larvae were reared through to the adult stage by providing fifth (last) instars (L5) with small cardboard cylinders to help them spin their cocoons. The following tissues were dissected from L4 and/or L5 larvae: brain (Br), Malpighian tubules (MT), midgut (MG), testes (Te), fat body (FB), epidermis (Ep), silk glands (SG), and CA. Brains were also dissected from newly molted pupae (P0) and newly emerged female moths.

Tissue was dissected under PBS and immediately transferred to 500 μL of RLT buffer for RNA extraction using the Qiagen QIAshredder and RNeasy Mini Kit (Qiagen). RNA was extracted from 40 pairs of CA each of L4 and newly molted L5 (L5D0) larvae, and from 5 to 20 brains, depending on the insect stage being sampled. Prior to extraction, 20 ng polyC RNA was added as carrier. For the other tissues/glands, RNA was extracted from material pooled from three animals. The concentration of total RNA (in water) was assessed in a 1-μL sample of each extract using a NanoDrop 1000 spectrophotometer (NanoDrop Technologies, DE). Reverse transcription was carried out for 1 h at 42°C, in 20 μL 1X-RT buffer containing 0.5 μg of an oligo$(dT)_{12–18}$ primer, 50 U SuperScript II RNase H^- reverse transcriptase (Invitrogen), and 0.5–1.5 μg total RNA, except for the CA samples whose reverse transcription reactions contained 30–35 ng RNA.

For quantitative real-time PCR (q-RT-PCR), four primers were initially designed for each of *Bm*FPPS-1 (BAB69490) and *Bm*FPPS-2 (BAAB01131085 and brP-0442 in *SilkBase*), as well as for *Bm*JHAMT (AB113578), another JH biosynthetic enzyme that was used as a positive control for the CA samples (this gene is preferentially expressed in the CA).[41] This redundancy provided four primer pair combinations for each gene, which were then used to assess primer pair performance and quantitative precision.

Preliminary amplifications conducted on pupal brain RNA generated similar transcript quantities for all four primer pair combinations for each individual gene, verifying gene-specific amplification. A single primer pair was then selected for each gene based upon high amplification efficiency and lack of nonspecific amplification products, which was then used for analysis of the remaining samples: *Bm*FPPS-1: 5′-GAAGAACAATTCGTGAGGTAGTCCCCTTGT-3′ and 5′-TACGGAGTCAATAAACCTGAAGCTATCGCC-3′; *Bm*FPPS-2: 5′-CTGGTAAAGTTGGTACAGATATACAAGAGCGC-3′ and 5′-GTCGTACATCGCTTTTTCTTGATGCTTGTATATCTGC-3′; *Bm*JHAMT: 5′-CCT-

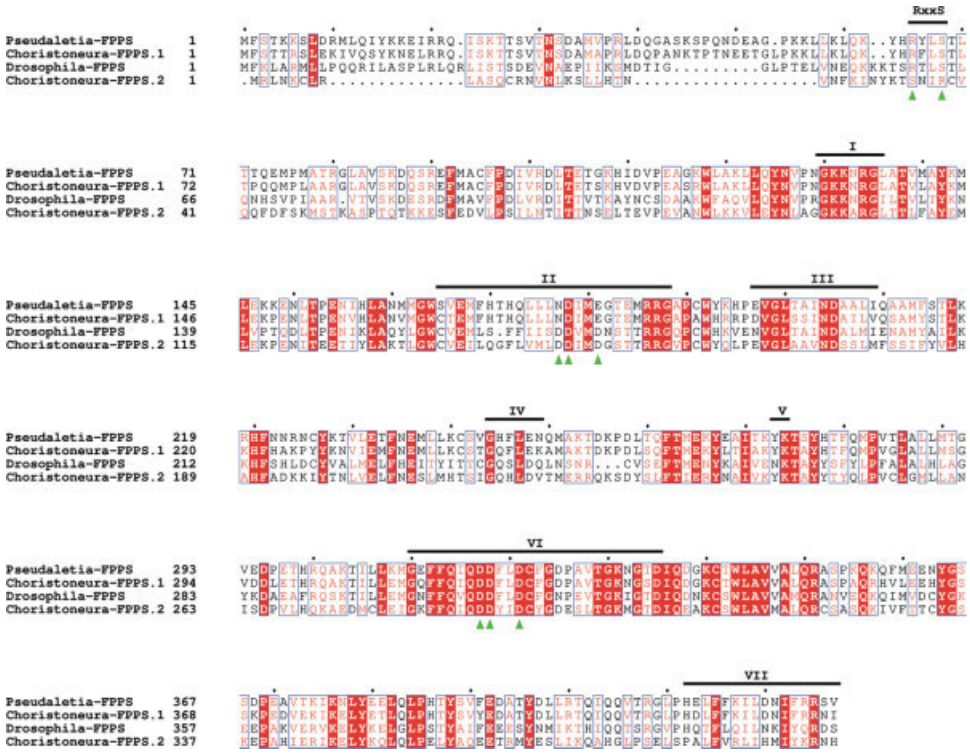

Fig. 2. ClustalW alignment of the amino acid sequences deduced from the three lepidopteran FPPS cDNAs cloned in this study and that of *D. melanogaster* (AAD27853); output generated by the program ESPript.[43] Green triangles indicate the positions of (i) the Arg and Ser residues within the putative mitochondrial targeting peptide cleavage motif, "RxxS"[44] and (ii) the Asp (or Asn or Glu) residues within the two aspartate-rich motifs. The lines under the Roman numerals span each of the seven prenyltransferase conserved regions identified by Koyama et al.[45]

AAGCAACACGCGTTGGCTTT-3′ and 5′-GTCAATAAATCC CGGGCAGGTTTCGTT-3′.

PCR amplifications were carried out on aliquots of individual RT reactions containing cDNA in amounts equivalent to 2–10 ng RNA, except for the CA samples, which contained amounts of cDNA equivalent to 0.16–0.17 ng RNA. Four replicate amplification reactions containing 500 nM of each primer were conducted for each sample using a MX3000P spectrofluorometric thermal cycler (Stratagene) and QuantiTect™ SYBR® Green PCR Kit (Qiagen), initiated with a 15-min incubation at 95°C, followed by a cycling regime of 95°C, 10 s; 65°C, 180 s. Each run was completed with a melting curve analysis to confirm the specificity of amplification and lack of primer dimers. Amplification efficiency was determined for each amplification reaction using sigmoidal analysis, and the number of target molecules calculated using lambda genomic DNA as a quantitative standard.[42]

RESULTS

Cloned FPPS cDNAs: Sequence Comparisons and Phylogenetic Analysis

The RT-PCR cloning approach that we employed yielded three lepidopteran cDNAs whose deduced amino acid sequences allowed their identification as FPPSs, as inferred from BLASTP analyses. A cDNA was generated from *P. unipuncta* CA mRNA and was named *Pu*FPPS (AY954921). A second cDNA, which was very similar to *Pu*FPPS, was cloned from *C. fumiferana* CF203 cells in culture, using an EST sequence (kindly provided by Q. Feng, Natural Resources Canada, Sault Ste. Marie, Ontario) as the starting point, and designated *Cf*FPPS-1 (AY954920). A third clone, clearly distinct from the first two and named *Cf*FPPS-2 (AY954919), was obtained from *C. fumiferana* adult brains. The amino acid sequences of these three proteins, along with that of *D. melanogaster* FPPS, a representative nonlepidopteran insect, are presented in Figure 2.

The *Pu*FPPS and *Cf*FPPS-1 cDNAs encode proteins of 427 (49.1 kDa) and 428 (49.0 kDa) amino acids, respectively, values that are almost identical to those reported for *Ai*FPPS[25] and *Bm*FPPS.[26] In comparison, *Cf*FPPS-2 is a smaller protein containing 397 amino acid residues (45.6 kDa). All of these proteins are larger than most noninsect FPPSs cloned so far, mainly as a result of long N-terminal extensions. In *Ai*FPPS, this extension was observed[25] to display features reminiscent of a mitochondrial transit peptide, as suggested by its amino acid composition and the presence of an RxxS sequence within the extension, which has been reported to be a mitochondrial targeting peptide cleavage motif.[44] Recent work has shown that the N-terminal extensions of *Ai*FPPS and *Dm*FPPS can indeed convey a reporter protein into yeast

mitochondria.[46] Among the sequences reported here, *Pu*FPPS and *Cf*FPPS-1 both contain an RxxS motif that aligns with that of *Dm*FPPS (see Fig. 2) as well as with those of *Ai*FPPS and *Bm*FPPS (not shown).

The seven conserved regions identified by Koyama et al.[45] are present in all three moth FPPSs reported here, including the two aspartate-rich motifs found in regions II and VI (see Fig. 2). However, the FARM of both *Pu*FPPS and *Cf*FPPS-1 displays two substitutions (DDxxD→NDxxE) that are also found in *Ai*FPPS and *Bm*FPPS, but not in *Cf*FPPS-2 (Table II). These substitutions are not observed in any other known FPPSs, across all groups of living organisms (see examples in Table II). FPPSs possessing the NDxxE motif (hereby defined as type-I lepidopteran FPPSs) also display two important substitutions at positions −5 and −4 relative to the FARM, where the two aromatic residues (Phe or Tyr) typically found in eukaryotic FPPSs[18,19] have been replaced by His and Gln, respectively (Table II). Interestingly, although most known eukaryotic FPPSs have two aromatic residues at these positions, those of many insects as well as those of unicellular organisms whose genomes have recently been sequenced do not. All nonlepidopteran insect FPPSs whose partial sequences are presented in Table II, with the exception of *Dm*FPPS and *Ips pini* FPPS, display a nonaromatic residue at either position −5 or −4 relative to the FARM. For example, the four partial FPPS cDNAs that we have cloned from aphids all encode a Gln at position −4. Similarly, *Cf*FPPS-2 and a related protein from *B. mori* (partial sequence gleaned from *B. mori* genomic and EST data bases) have Leu and Cys residues at position −4 (Table II).

In a multispecies comparison that included only those insect FPPSs for which a full sequence is available, the highest degree of amino acid identity and similarity was observed among the four lepidopteran enzymes with the HQxxxNDxxE signature motif (Table III). Not surprisingly, *Pu*FPPS and *Ai*FPPS displayed the greatest degree of identity (94%) since both genera belong to the same family (Noctuidae). The protein of the more distantly related *B. mori* (Bombycidae) showed 83% identity to those of the two noctuids, and that of the tortricid *C. fumiferana* (*Cf*FPPS-1), a more primitive group,[47] showed identities of 79–80% relative to the other three. Surprisingly, these four proteins displayed lower degrees of identity to the second FPPS from *C. fumiferana* (*Cf*FPPS-2) than to nonlepidopteran insect FPPSs (Table III).

Several of the above observations are reflected in the phylogenetic tree that we constructed using the same insect FPPS sequences as well as that of a second *Bm*FPPS (see "type-II" lepidopteran FPPSs in Table II) and those of selected noninsect organisms (see Fig. 3). All insect FPPSs are seen to form a cluster distinct from vertebrate and plant enzymes, within which lepidopteran (HQxxxNDxxE), coleopteran, homopteran, and dipteran FPPSs form separate subclusters. Interestingly, *Cf*FPPS-2 and *Bm*FPPS-2 form a separate cluster adjacent to the other insect FPPSs, suggesting a gene duplication event that took place in an ancestor of all insect groups considered here. Among the noninsect eukaryotic FPPSs, the vertebrate proteins form a well-supported group adjacent to the insect FPPSs. Those of nematode, nonanimal eukaryotes, bacteria, and archaea cluster at the opposite end of the unrooted tree from the insect FPPSs and show no patterns of relationships with each other, likely owing to the lack of taxonomic sampling (see Fig. 3).

Structure and Organization of the *Cf* FPPS-1 and *Cf* FPPS-*2* Genes

In an effort to gain a better understanding of the evolutionary relationship existing between the two FPPS homologs that we cloned from *C. fumiferana*, we initiated an analysis of the structure of their respective genes. The *Cf*FPPS-1 (AY962308 and AY962309) and *Cf*FPPS-2 (AY962307) genes display a very similar organization, each containing six exons, of which the last four are of identical size (see Fig. 4). In accord with its small size, the two 5′-end exons of *Cf*FPPS-2 are shorter than those of *Cf*FPPS-1, and the sequence identity between the two genes is lower for exons 1 and 2 (44 and 46%, respectively) than it is for the remaining exons (52–60%; Fig. 4). In comparison, the genomic sequences of *Cf*FPPS-1 and *Bm*FPPS (referred to here as *Bm*FPPS-1; see type-I lepidopteran FPPSs in Table II) show an identical exonic structure, with a single codon insertion in exon 1 of *Cf*FPPS-1 (Leu54; Fig. 2).

A partial genomic sequence (exons 2–6 and introns) was extracted from data bases for the putative type-II *Bm*FPPS (referred to here as *Bm*FPPS-2). As with *Cf*FPPS-2, this sequence contains the standard DDxxD FARM motif (Table II), and exons 3–6 are similar in size to those of the other three lepidopteran FPPSs shown in Figure 4. Exon 2, however, is larger (219 vs 160–169 nt). The *Dm*FPPS gene also contains six exons but displays markedly different splicing junctions, relative to the lepidopteran genes (see Fig. 4). In all comparisons among lepidopteran and *D. melanogaster* FPPS genes, introns varied widely in size, and none showed significant sequence identity.

Assessment of FPPS Functionality: Yeast Complementation Assay

Our efforts to carry out in vitro enzyme assays using recombinant insect FPPSs produced in a bacterial expression system have met with several difficulties. Although r*Dm*FPPS-His proved to be reasonably stable and active (in vitro characterization of this enzyme to be reported elsewhere) when assayed under conditions similar to those described earlier,[14] the recombinant lepidopteran enzymes tended to lose most, if not all, of their activity during the purification steps. This did not come as a complete surprise inasmuch as the remarkable lability of lepidopteran FPPSs had been noted earlier,[14,48] and because replacement of one or more aspartates within the FARM of eukaryotic FPPS is known to result in diminished catalytic activity.[49,50] In an attempt to circumvent this prob-

TABLE II. Alignment of Amino Acid Residues of Insect and Other Eukaryotic FPPSs Within Selected Portions of the Conserved Regions Identified by Koyama et al.[45]

			Portions of FPPS conserved regions				
Eukaryotic type	Group	Species	II	III	*	IV	V+
			DDxx**D**				
Multicellular, noninsect	Mammal	*Homo sapiens*[1]	**L**QA**FF**LVA**DD**IM**D**	INDAN	**S**YQT**E**I	G**Q**TL**D**L	KTAF**Y**
	Mammal	*Rattus norvegicus*[2]	**L**QA**FF**LVL**DD**IM**D**	INDAN	**S**YQT**E**I	G**Q**TL**D**L	KTAF**Y**
	Bird	*Gallus gallus*[3]	**F**QA**FF**LVA**DD**IM**D**	INDS**F**	**A**YQT**E**L	G**Q**ML**D**L	KTAF**Y**
	Nematode	*Caenorhabditis elegans*[4]	**I**QS**FY**LIA**DD**IM**D**	INDA**F**	KQKTLI	G**QF**L**D**T	KTSH**Y**
	Yeast	*Saccharomyces cerevisae*[5]	LQAYFLVADDMMD	INDA**F**	**T**FQT**E**L	G**Q**LM**D**L	KTAY**Y**
	Plant	*Arabidopsis thaliana*[6]	**L**QA**YF**LVL**DD**IM**D**	INDG**I**	EFQTAC	G**Q**MI**D**L	KTAY**Y**
Unicellular	Alveolata	*Plasmodium falciparum*[7]	**L**QA**SF**LVA**DD**IM**D**	VNDV**F**	**T**LKTIV	G**QH**L**D**T	KSAY**Y**
	Euglenozoa	*Trypanosoma cruzi*[8]	**L**QA**HY**LVE**DD**IM**D**	INDG**I**	DYATAV	G**Q**MY**D**V	KTTF**Y**
Insect, nonlepidopteran	Diptera	*Drosophila melanogaster*[9]	**L**.S**FF**IIS**DD**VM**D**	INDA**L**	**T**YITTC	G**Q**SL**D**Q	KTAY**Y**
	Diptera	*Anopheles gambiae*[10]	**L**HS**MF**LIM**DD**VM**D**	VNDA**I**	KFITTI	G**Q**SL**D**L	KTAY**Y**
	Hemiptera	*Myzus persicae*[11]	**L**QA**YQ**LVL**DD**IM**D**	VNDG**V**	**T**MKTAM	G**Q**CL**D**M	KTAY**Y**
	Hemiptera	*Acyrtosiphon pisum*[12]	**L**QA**YQ**LVL**DD**IM**D**	VNDG**V**	**T**MKT**S**M	G**Q**CL**D**M	KTAY**Y**
	Hemiptera	*Aphis fabae*[13]	**L**QA**YQ**LVL**DD**IM**D**	VNDG**I**	**T**MKT**S**M	G**Q**CL**D**M	KTAY**Y**
	Hemiptera	*Megoura viciae*[14]	**L**QA**YQ**LVL**DD**IM**D**	VNDG**I**	**A**MKTAM	G**Q**CL**D**M	KTAY**Y**
	Coleoptera	*Ips pini*[15]	**L**HT**YF**LII**DD**II**D**	VYDA**V**	**A**LKT**S**L	G**Q**SL**D**T	KTSY**Y**
	Coleoptera	*Dendroctonus jeffreyi*[16]	**V**HA**YV**LIL**DD**IM**D**	VNDA**V**	NLKTTL	G**Q**SL**D**A	KTAF**Y**
	Coleoptera	*Anthonomus grandis*[17]	**I**HS**CF**LVL**DD**IM**D**	INDG**L**	VSKTTL	G**Q**CL**D**S	KTAY**Y**
	Hymenoptera	*Apis mellifera*[18]	**M**QA**FH**TMI**DD**IL**D**	INDG**L**	**T**IEKY-	—	—
Insect, lepidopteran	Type II	*Choristoneura fumiferana*[19]	**L**QG**FL**VML**DD**IM**D**	VNDS**S**	**L**MHT**S**I	G**QH**L**D**V	KTAY**Y**
	FARM=**DD**IM**D**	*Bombyx mori*[20]	**F**QA**YC**IVL**DD**IM**D**	FNDS**L**	**L**WRT**S**M	G**QH**L**D**H	KAAY**Y**
	Type I	*Pseudaletia unipuncta*[21]	**F**HT**HQ**LLL**ND**IM**E**	INDA**A**	**L**LKC**S**V	G**HF**L**E**N	KTSY**H**
	FARM=**ND**IM**E**	*Agrotis ipsilon*[22]	**F**HT**HQ**LLL**ND**IM**E**	INDA**A**	**L**LKC**S**I	G**HF**L**E**N	KTSY**H**
		Bombyx mori[23]	**F**HT**HQ**LLL**ND**IM**E**	INDA**A**	**L**MKC**S**M	G**HY**V**Q**K	KTSY**Y**
		Choristoneura fumiferana[24]	**F**HT**HQ**LLL**ND**IM**E**	INDA**I**	**L**LKC**S**T	G**QF**L**E**K	KTAY**H**
		Numbering**	**a..bc...de..f**	**....g**	**h...i.**	**.j..k.**	**....l**

*The six amino acid residues immediately preceding region IV.

Lepidopteran (*P. unipuncta*)/avian (*G. gallus*) numbering: **a: 169/109; **b**: 172/112; **c**: 173/113; **d**: 177/117; **e**: 178/118; **f**: 181/121; **g**: 207/147; **h**: 238/178; **i**: 242/182; **j**: 245/185; **k**: 248/188; **l**: 278/218.

Symbols: . = gap; — = unsequenced portion; FARM: First Aspartate-Rich Motif.

Sequence sources: (1) AAH10004; (2) NP_114028; (3) P08836; (4) NP_493027 (5) P08524; (6) AAB07248 ; (7) AA063552; (8) AAK71861; (9) AAD27853; (10) XP_308653; (11) AY968586; (12) AY968585; (13) AY968583; (14) AY968584; (15) AY953507; (16) AY966009; (17) AY966008; (18) XP_396224; (19) AY954919; (20) BAAB01131085 and SilkBase brP-0442; (21) AY954921; (22) CAA08918 ; (23) BAB69490; (24) AY954920.

DOI 10.1002/prot

TABLE III. Amino Acid Identity (Right of Diagonal) and Similarity (Left of Diagonal) Among Known Insect FPPSs

	Pu	Ai	Bm	Cf1	Mp	Ag	Dm	Cf2
Pseudaletia unipuncta	·	94	83	80	51	48	46	43
Agrotis ipsilon	96	·	83	79	51	48	48	43
Bombyx mori-1	90	91	·	79	54	49	48	45
Choristoneura fumiferana-1	90	89	89	·	51	49	49	44
Myzus persicae	72	72	74	72	·	59	53	43
Anthonomus grandis	69	70	71	70	77	·	54	41
Drosophila melanogaster	67	69	69	71	71	72	·	40
Choristoneura fumiferana-2	64	67	67	66	63	61	62	·

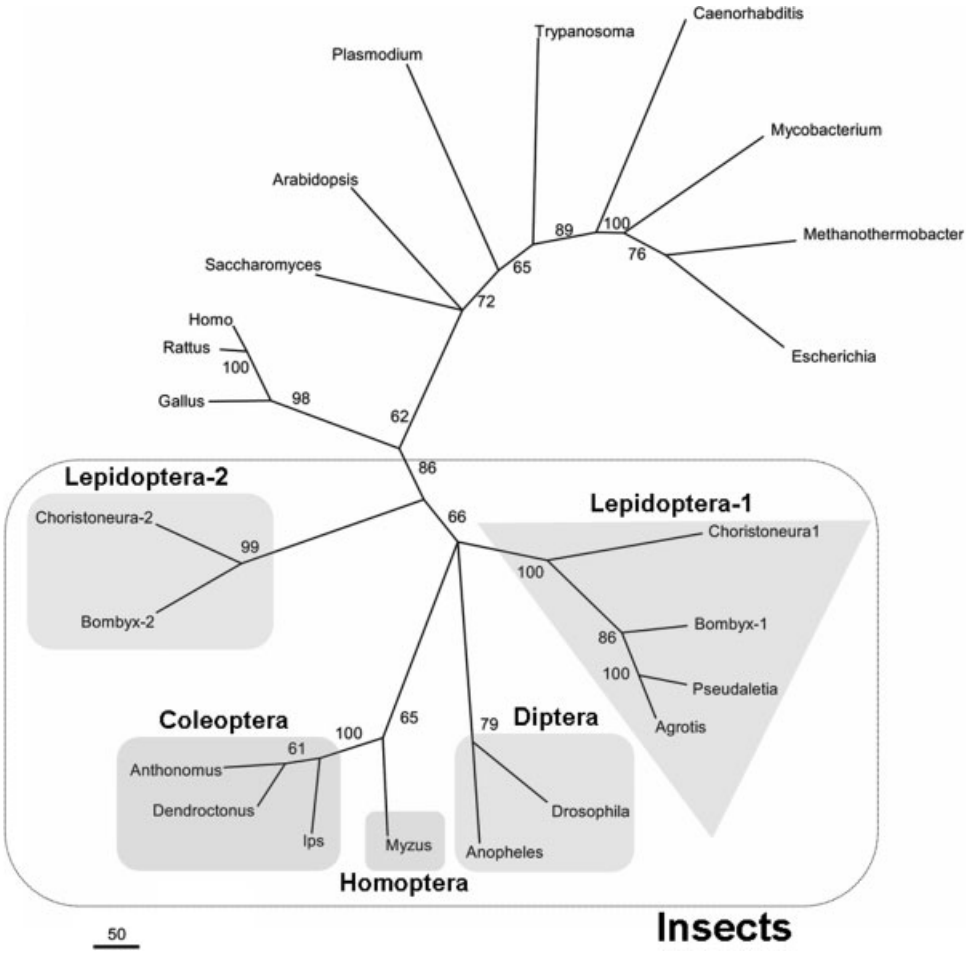

Fig. 3. Unrooted phylogram generated for selected farnesyl diphosphate synthases (FPPSs). The amino acid sequences were aligned using ClustalX[35] and analyzed heuristically in PAUP*[36] using parsimony optimality criterion with informative characters treated as unordered and unweighted. Numbers at the nodes are bootstrap values calculated for 10,000 pseudoreplicates. The scale bar refers to 50 amino acid changes per unit length. Full species names and GenBank accession numbers for the eukaryotic FPPS sequences are given in Table II, while those for the three prokaryotic FPPS sequences are: *Methanothermobacter thermoautotrophicum*, AAB32421; *Escherichia coli*, NP 414955; *Mycobacterium tuberculosis*, NP 217900.

lem, we assessed FPPS functionality of the cloned enzymes using a yeast complementation assay. To this end, we employed the CC25 *S. cerevisae* "leaky" mutant,[32] which shows growth inhibition in the absence of ergosterol (an end product of the FPP pathway). The CC25 mutant transformed with a vector containing the *Dm*FPPS ORF generated a growth curve, in the absence of ergosterol, almost identical to that observed with the control mutant cultured in the presence of ergosterol. However, mutant yeast expressing the lepidopteran FPPSs, in the absence of ergosterol, all grew less rapidly, albeit significantly better than control yeast (see Fig. 5).

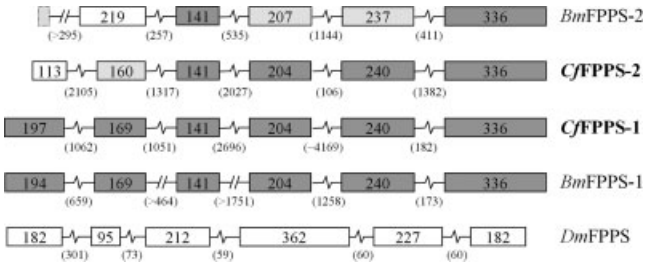

Fig. 4. Exon and intron splicing junctions (from start to stop codons) of the two putative *C. fumiferana* FPPS genes cloned in this study, along with those of two homologous genes from *B. mori* (*Bm*FPPS-1: BAAB01029497, BAAB01034558 and BAAB01199140; *Bm*FPPS-2: BAAB01131085) and that of *D. melanogaster* (AE003826; FBgn0025373). Numbers in boxes are the number of bp in each exon (boxes drawn to scale); numbers in brackets are the numbers of bp in each intron (approximate value in *Cf*FPPS-1: short DNA stretch that could not be successfully sequenced). For the *B. mori* sequences, complete data could not be obtained for all introns, and no contig containing the first exon of *Bm*FPPS-2 (light grey) could be found in the data base. Solid grey boxes: identical or nearly identical exon lengths among aligned exons; these exons show clear homology. Light grey boxes: similar exon length among aligned exons; the level of nucleotide identity among these exons is lower than that seen among the exons shown in solid grey. Open boxes: limited or no clear relationship with exons in the same sequential position in the other FPPS genes.

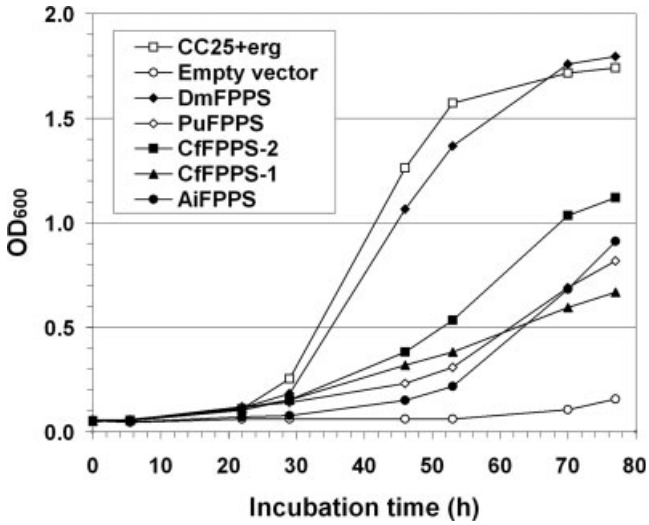

Fig. 5. Growth curves generated for the CC25 FPPS yeast mutant, with or without complementation with one of several insect FPPS cDNAs. Growth at 28°C was monitored by measuring OD_{600} at different intervals following inoculation of culture medium. Open boxes: control (uncomplemented) yeast mutant in the *presence* of ergosterol and uracil (CC25+erg). The remaining curves were generated by growing yeast in the *absence* of ergosterol and uracil: solid diamonds, complementation with *D. melanogaster* FPPS cDNA; solid circles, complementation with *A. ipsilon* FPPS cDNA; open diamonds, complementation with *P. unipuncta* FPPS cDNA; solid boxes, complementation with *C. fumiferana* FPPS-2 cDNA; solid triangle: complementation with *C. fumiferana* FPPS-1 cDNA; open circles, CC25 yeast transformed with empty vector. The vector carries a gene essential for the synthesis of uracil and, thus, essential for yeast growth. Therefore, the open-circle curve represents the background growth of this "leaky" mutant. Each point is the average of at least three independent measurements.

Structural Analysis of Amino Acid Substitutions in the Active Site of Lepidopteran FPPSs

In an attempt to determine whether substitutions specific to lepidopteran FPPSs could facilitate binding of the bulkier ethyl-branched substrates and products that are precursors of JHs, we developed a computational model for the catalytic cavity of one of these enzymes. We initially focused on the type-I enzymes given that two of these cDNAs were generated from CA RNA (*Pu*FPPS, this study; *Bm*FPPS-1[26]) and that their active site had accumulated more substitutions than that of type-II FPPSs, as compared with other nonlepidopteran, eukaryotic FPPSs (see Table II). For this purpose, we built a homology model of *Pu*FPPS, assuming a homodimeric composition similar to that of the avian FPPS template, and conducted docking simulations with several homologous FPP products.

The Asp→Asn (N177) and Asp→Glu (E181) substitutions within the FARM constitute the most readily noticeable feature of type-I lepidopteran FPPSs, given the perfectly conserved nature of the DDx(xx)xD motif among the FPPSs of all other organisms examined to date (Table II) and the demonstrated roles of these Asp residues in both binding of the allylic substrate/product and catalysis.[49,50] Interestingly, although the second DDxxD motif is intact in these proteins, an additional Asp→Glu (E248) substitution (Gln in *Bm*FPPS-1; see 5th residue in region IV, Table II) is observed on α-helix F, near the FARM, which is located on α-helix D (Figs. 6 and 7). These substitutions appear to cause a shift in the position of the Mg^{2+} ion toward the carboxyl groups of Glu181 and Glu248, which is likely to affect binding of the allylic ligand through the Mg^{2+} ion and, as a consequence, the general orientation of the ligand within the active site, a prediction that is supported by the results of docking simulations (see Fig. 7).

The Phe→His (H172) and Phe→Gln (Q173) substitutions, at positions −5 and −4 relative to the FARM, respectively, are also very distinctive given that eukaryotic FPPSs typically display two uncharged aromatic residues (Phe or Tyr) at these positions (Table II) and that their role in determining product chain length specificity has been demonstrated through site-directed mutagenesis.[21,51–53] In considering the possible formation of ethyl-substituted products, however, these two substitutions, along with Phe→Ala (A207′) and Glu→Ser (S242), would likely contribute to an increase in the volume of the catalytic cavity in the vicinity of the bottom wall, thereby facilitating formation of FPP derivatives bearing an ethyl group at their ω end (see Fig. 8). Residues on α-helix E of one subunit of the homodimer, including Ala207′ (lepidopteran structure) and Phe147′ (avian structure), may also affect the size of the catalytic cavity in the other subunit inasmuch as both α-helix E and the bottom wall of the active site are at the dimer interface[54] (see Fig. 6). While not all nonlepidopteran FPPSs have a Phe residue at this position, most of them display a bulky hydrophobic amino acid (see bold letters in region III, Table II).

Given the apparent "opening" of the floor of the catalytic cavity seen in type-I lepidopteran FPPS (see Fig. 8), the question arises as to what other structural feature(s) could provide termination of chain elongation to produce the larger FPP products. Leu238 and Phe169 (see Fig. 8) are two candi-

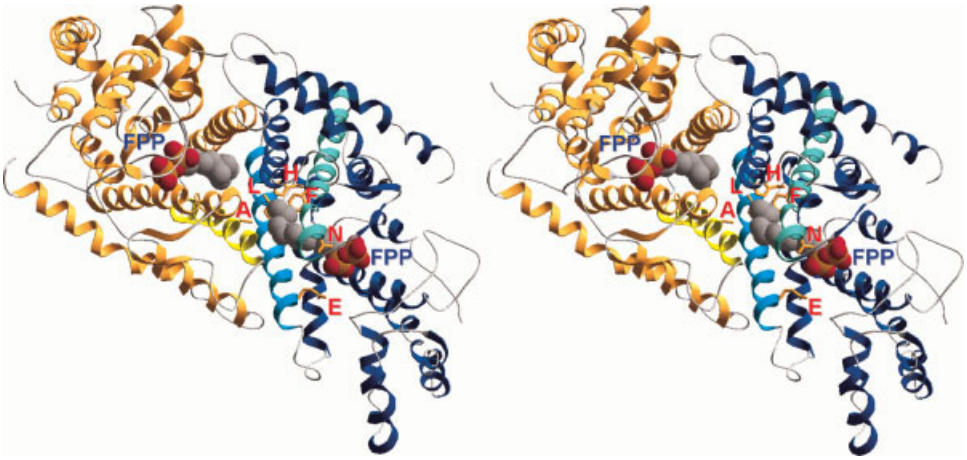

Fig. 6. Stereo view of a type-I lepidopteran FPPS dimer (homology model) in ribbon rendering, with bound FPP (space-fill, grey with red and yellow diphosphate). In the subunit displayed in blue, α-helices D and F are shown in sky blue and royal blue, respectively. In the subunit displayed in orange–yellow, α-helix E is shown in bright yellow. Side-chains of selected amino acid residues are displayed in orange–yellow (A: Ala207′; E: Glu248; F: Phe169; H: His172; L: Leu238; N: Asn177).

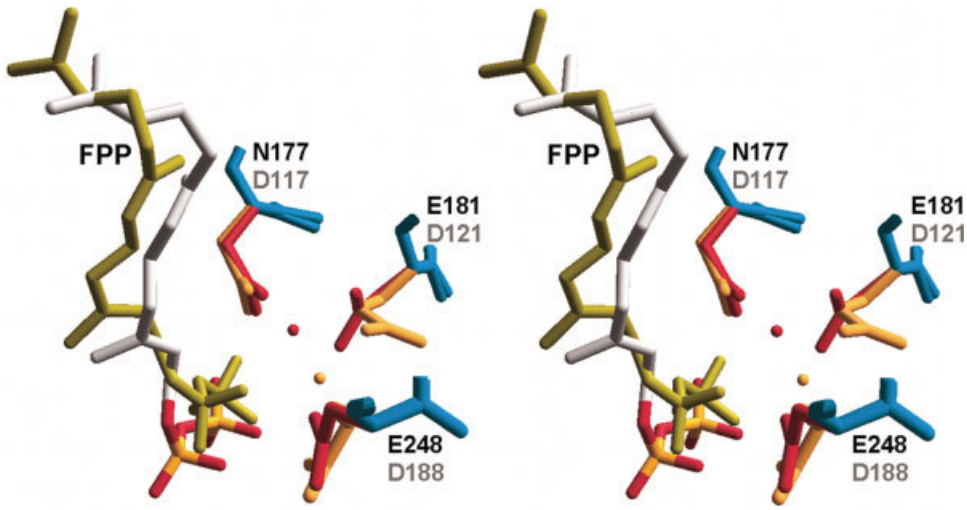

Fig. 7. Stereo view of superimposed lepidopteran (homology model) and avian (1UBX, with A112F/S113F) FPPS structures, highlighting potential impact of Asp substitutions within the first aspartate-rich motif (FARM) upon binding of allylic ligand through Mg^{2+} ions (red and yellow balls for avian and lepidopteran FPPSs, respectively). Yellow side chains and black numbering: lepidopteran FPPS; red side chains and grey numbering: avian FPPS. The ligand, FPP, is shown in its final position within the active site of each FPPS (yellow-green: lepidopteran; white and red/yellow: avian) at the end of a docking simulation using the *Eve* algorithm. Energy minimization of the lepidopteran FPPS structure resulted in a shift of the Mg^{2+} ion toward Glu181 and Glu248. The latter is on α-helix F, which is on the opposite side of the catalytic cavity relative to the FARM (on α-helix D; see Fig. 6).[20] The three Asp substitutions shown here and the resulting shift in the Mg^{2+} ion may play a role in the overall orientation of the ligand within the active site. Note that the ω end of FPP (top of picture) reaches further "down" in the active site of the lepidopteran structure than in that of the avian protein.

dates given that residues at equivalent positions have been shown to play a role in product chain length selectivity of other prenyl transferases.[55–57] The product apparently descends deeper in the catalytic cavity of type-I lepidopteran FPPS than it does in the avian enzyme (see Figs. 7 and 8).

With respect to the formation of bis- and trishomo-FPP, which are the precursors of JH I and JH 0, respectively, we have identified two substitutions, Gln→His (H245) and Tyr→His (H278), which could provide the structural environment that the additional ethyl branches of BHFPP and THFPP would require (see Fig. 8). It should be noted, however, that *Bm*FPPS-1 lacks the Tyr→His substitution while *Cf*FPPS-1 lacks the Gln→His substitution (see regions IV and V+, Table II).

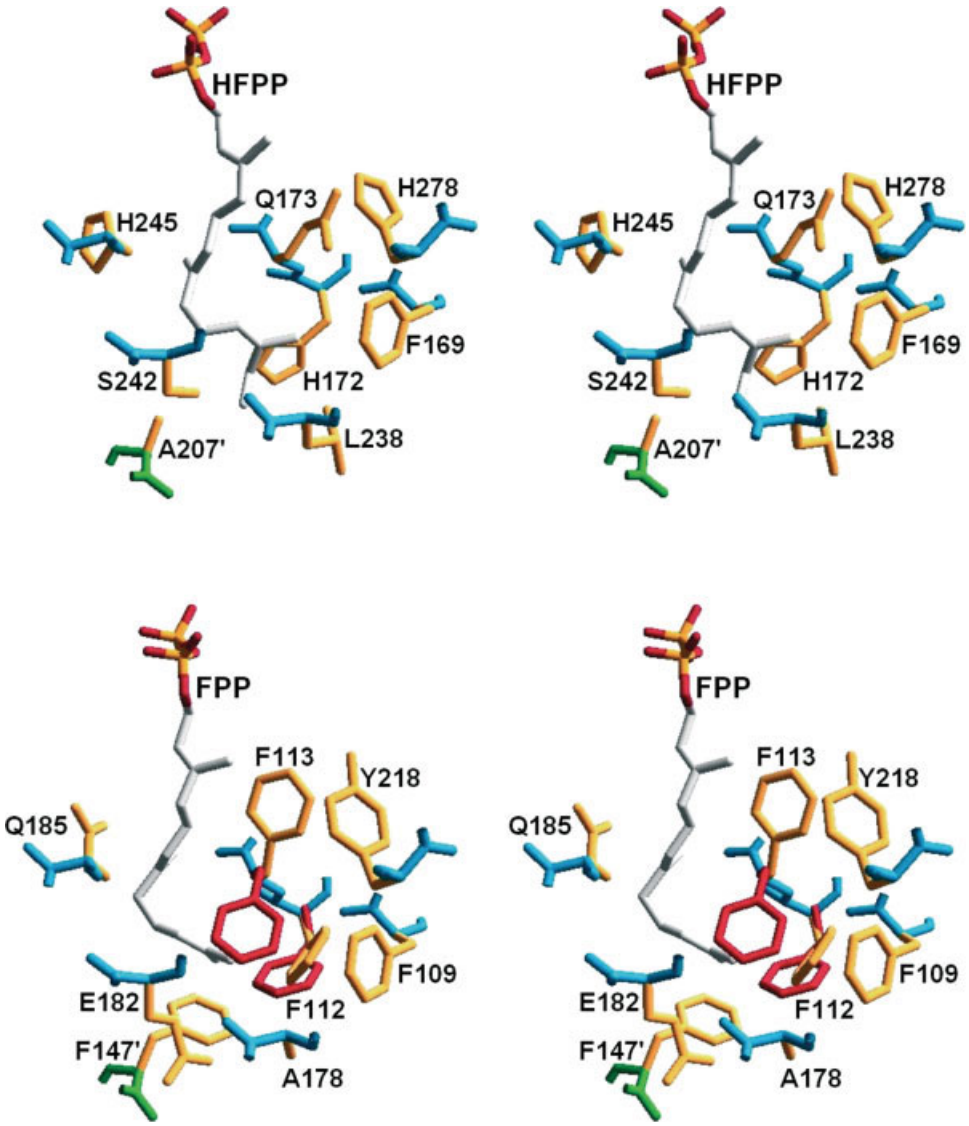

Fig. 8. Stereo view of type-I lepidopteran (homology model; top panel) and avian (1UBX with A112F and S113F; lower panel) FPPS structures, highlighting substitutions likely to have an impact on active site volume. Ala207′ (lepidopteran) and Phe147′ (avian) are on α-helix E (see Fig. 6) of the other subunit (green backbone). The lepidopteran and avian structures are shown with bound homo-FPP (HFPP) and FPP, respectively, in their final positions at the end of a docking simulation using the *Eve* algorithm. Energy minimization of the 1UBX structure following conversion of the Ala112/Ser113 residues to Phe resulted in an orientation of the side chain of Phe113 (yellow) that is not in agreement with its role in product chain-length determination.[21] The exact conformations of Phe112 and Phe113 in the native liganded protein is unknown; we show here the position of their side chains in the superimposed apoprotein 1FPS (red, lower panel).

In comparison with type-I lepidopteran FPPSs, the active-site residues of the two type-II FPPSs presented here show strong similarity to those of the avian enzyme and other nonlepidopteran eukaryotic FPPSs (Table II). Possible exceptions include the residue at position −4 relative to the FARM, which is a Leu in *Cf*FPPS-2 and a Cys in *Bm*FPPS-2, and the Leu and Ser residues within the six-residue segment immediately upstream of region IV (the latter substitutions being common for both type I and type II lepidopteran FPPSs; Table II). It should be noted, however, that these substitutions can be observed in several FPPSs of nonlepidopteran insects (Val113 in *D. jeffreyi* FPPS and Ser182 in three aphid FPPSs, avian numbering; Table II) and that the Ala–Leu substitution is not expected to cause an increase in the volume of the catalytic cavity. The His residues within region IV (shown in bold letters in Table II) are expected to have their side chains turned away from the active site, as inferred from the avian structure (not shown).

In docking simulations comparing the *Pu*FPPS model and avian FPPS structure, scores obtained for the four different FPP homologs tested revealed a significant dif-

TABLE IV. Comparative Scores (kcal/mol) for Four Ligands [FPP, homo-FPP, bishomo-FPP, trishomo-FPP; see Fig. 1(B)] Docked in the Active Site of a Type-I Lepidopteran FPPS (Homology Model) and Avian FPPS (1UBX With A112F and S113F) Using the *Eve* Algorithm

Ligand	Lepdiopteran FPPS	Avian FPPS
Farnesyl diphosphate (FPP)	−60.97	−40.85
Homo-farnesyl diphosphate (homo-FPP)	−63.91	−18.83
Bishomo-farnesyl diphosphate (bishomo-FPP)	−65.48	Not in site
Trishomo-farnesyl diphosphate (trishomo-FPP)	−69.11	Not in site

ference in binding to lepidopteran and nonlepidopteran active sites. Using the lepidopteran model as target, FPP and each of its homologs displayed similar affinities, with a modest inverse relationship seen between binding energy and the level of ethyl substitution of the diphosphate products. When the avian structure was used as target, a 20 kcal/mol difference in binding energy was seen between FPP and homo-FPP, and neither bis- nor trishomo-FPP could dock successfully in the active site (Table IV).

Tissue-Specific Transcription of *Bm*FPPS-1 and *Bm*FPPS-2

To explore the contribution of each of the two lepidopteran FPPS types to JH biosynthesis and other metabolic pathways, we assessed the abundance of transcripts encoding *Bm*FPPS-1 and *Bm*FPPS-2 in various tissues of the silkworm, *B. mori*, including the CA. The choice of the silkworm to conduct this experiment, instead of *C. fumiferana*, was based strictly on practical considerations, *B. mori* caterpillars being significantly larger than those of *C. fumiferana*, thus making it easier to dissect the very minute larval CA.

*Bm*FPPS-1 transcript abundance varied between ~3000 and 60,000 per 10 ng RNA, depending on the tissue examined, but the levels measured in the CA were not as high (~12,000–15,000) as those observed in brains (L5, P0, and adults), Mapighian tubules, and testes (see Fig. 9). Against our expectations, however, *Bm*FPPS-2 transcripts were rare in all tissues sampled (<300 per 10 ng RNA), except in the CA where they reached levels of >260,000 per 10 ng RNA in both fourth and newly molted fifth-stadium larvae (see Fig. 9). *Bm*JHAMT transcript levels (data not shown) displayed a tissue distribution identical to that reported earlier for *B. mori*,[41] thus validating the accuracy of our quantitative assessments of *Bm*FPPS-1 and *Bm*FPPS-2 transcript abundance.

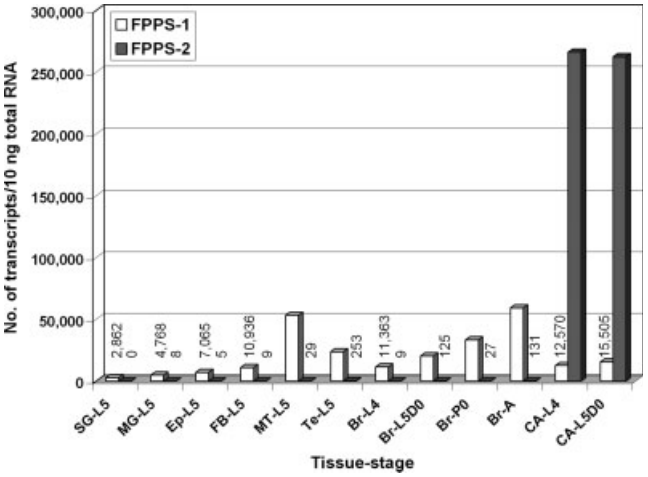

Fig. 9. Assessment of *Bm*FPPS-1 and *Bm*FPPS-2 transcript abundance in selected *B. mori* tissues, as determined by quantitative real-time PCR. Tissues sampled: Br, brain; CA, corpora allata; Ep, epidermis; FB, fat body; MG, midgut; MT, Malpighian tubules; Te, testes; SG, silk glands (whole). Stages: L4, fourth instars; L5, fifth instars (any age); L5D0, newly molted fifth instars; P0, newly molted pupae; A: adults (newly emerged females). Actual transcript numbers are provided above each bar for all values <20,000.

DISCUSSION

Our main goal in undertaking the present work was to determine whether lepidopteran CA express a unique form of FPPS, adapted for the production of the ethyl-branched FPP precursors of JH 0, JH I, and JH II. The existence of such a specialized prenyltransferase was inferred from results of in vitro FPPS assays carried out on *M. sexta* CA homogenates, which revealed a selectivity of the CA enzyme for ethyl-substituted substrates.[14,15] Two closely related lepidopteran FPPS cDNAs had previously been cloned from *A. ipsilon*[25] and *B. mori*,[26] and both encoded an enzyme displaying singular active site substitutions not previously observed in any other eukaryotic FPPS, including that of the dipteran *D. melanogaster*. Although the *Ai*FPPS cDNA was obtained from brain RNA, RNase protection assays comparing the expression of this gene in various *A. ipsilon* tissues had led to the conclusion that it was preferentially expressed in the CA.[25] Conversely, the related *Bm*FPPS cDNA was cloned from larval CA RNA, but semiquantitative RT-PCR analysis indicated that its expression was ubiquitous.[26]

Here, we report on the cloning and characterization of three cDNAs and the analysis of two distinct forms of lepidopteran FPPS, which we have defined as type-I and type-II FPPSs. Two of these cDNAs encode proteins (*Cf*FPPS-1 and *Pu*FPPS) clearly related to previously reported lepidopteran FPPSs, sharing a distinctive HQxxxNDIME (type I) signature motif. The third cDNA encodes a protein (*Cf*FPPS-2) representing a new type of lepidopteran FPPS (type II) for which we found a homologous sequence in *B. mori* genomic and EST data bases.

In the phylogenetic tree presented here, the two representatives of type-II lepidopteran FPPS form a distinct cluster relative to all other known insect FPPSs, including the four known lepidopteran type-I enzymes (see Fig. 3). The similarity in the gene structure of the two

lepidopteran FPPS types suggests that they originated from a gene duplication event, after which significant divergence occurred, particularly in the exons encoding the N-termini (see Fig. 4). Whether the duplication event occurred in an ancestor of all insect groups considered here, as the present phylogram suggests (see Fig. 3), or in a lepidopteran ancestor of the primitive *C. fumiferana*, needs to be assessed through a comparison of many additional insect FPPS sequences and gene structures. These additional data would also help determine whether the FPPS dichotomy reported here is truly representative of all Lepidoptera.

In trying to predict which of the two lepidopteran FPPS types could have evolved a specialized function in the biosynthesis of ethyl-branched JHs, the present phylogenetic analysis (see Fig. 3) suggested that the more divergent type-II enzyme was the stronger candidate. However, this prediction needed to be weighed against two independent observations. First, two type-I FPPS cDNAs were generated from CA RNA whereas the two type-II FPPS cDNAs were obtained from brain RNA (*Cf*FPPS-2: adult brains; *Bm*FPPS-2: day-0 pupal brains). Second, the structural analysis reported here indicates that the type-I enzyme has accumulated more amino acid substitutions within its catalytic cavity than the type-II protein, which displays more "conventional" active site residues. Docking simulations involving ethyl-substituted FPP derivatives as ligands and a homology model of a type-I FPPS as target suggest that this enzyme's active site has structural features allowing it to bind ethyl-substituted substrates and products better than would a more "conventional" form of this enzyme, such as chicken FPPS.

In view of the above considerations, it became imperative to assess transcript distribution for each of the two FPPS types in insect tissues. The results of our q-RT-PCR assays, which focused on the transcription of *Bm*FPPS-1 and *Bm*FPPS-2 in *B. mori*, offer a striking picture of the likely involvement of each FPPS homolog in JH biosynthesis. Expression of *Bm*FPPS-2 was observed to be essentially confined to the CA, in a manner similar to that shown earlier for another JH biosynthetic enzyme, *Bm*JHAMT,[41] whereas *Bm*FPPS-1 was expressed in all tissues examined (see Fig. 9), as reported by another group using an alternative method.[26] Furthermore, although *Bm*FPPS-1 transcripts were not rare in CA tissue, those of *Bm*FPPS-2 were ~20 times more abundant. Although we cannot exclude, on the basis of these results, the involvement of the type-I enzyme in JH biosynthesis, the almost exclusive expression of type-II FPPS transcript within the CA (although we did not assay all possible tissues) strongly argues for a role in JH production, particularly since these endocrine glands have few other known biochemical functions. The actual contribution of each FPPS homolog to lepidopteran JH biosynthesis will need to be examined using gene silencing methods combined with in vitro measurements of JH release rates.[58] Similar quantitative analyses should also be conducted on other lepidopteran species, as well as on adult tissues, given that the work that reported preferential expression of *Ai*FPPS in the CA was carried out in moths.[25]

The tissue distribution of type-I and type-II FPPS transcripts in *B. mori* (see Fig. 9) raises questions as to how the cDNAs of *Bm*FPPS-2 and *Cf*FPPS-2 could have been cloned from pupal and adult brains, respectively, using a standard RT-PCR approach and degenerate primers, when these two tissue sources were shown to contain ~400–1000 times more FPPS-1 than FPPS-2 transcripts, at least in the silkworm. A similar question arises regarding the cloning of type-I FPPS cDNAs from larval CA (*Bm*FPPS-1) and adult CA (*Pu*FPPS). Regarding the cloning of the type-II FPPS cDNAs, there may be a simple explanation in that the CA often remain attached to the brain during tissue extirpation. However, the q-PCR results presented here were performed with dissected brains that were carefully cleaned to remove all extraneous tissue, including the CA. With respect to the cloning of *Bm*FPPS-1 and *Pu*FPPS from CA RNA, it must be pointed out that *Bm*FPPS-1 transcripts, although less abundant than their type-II counterpart, are not rare in larval *B. mori* CA, and the choice of primers and/or the existence of different secondary sructures in the two FPPS transcripts could have favored the amplification of one cDNA to the detriment of the other.

As indicated above, the strong predominance of the *Bm*FPPS-2 transcript in *B. mori* CA suggests that this form of the enzyme could play a leading role in the biosynthesis of the ethyl-branched JHs, at least in larvae. Based on an analysis of the enzyme's active site alone, the type-II FPPSs certainly appear less well suited for handling the bulkier ethyl-substituted substrates and products than the type-I enzymes. However, several recent studies have shown that substitutions in amino acid residues that have no direct contact with the ligand can have substantial effects on substrate specificity.[59,60] In this context, it is important to note that the type-I and type-II enzymes display significant differences in residues located at some distance from the catalytic cavity, including those of the N-termini, which differ in both length and composition (see Fig. 2). In addition, the homology model presented here was developed using a template that lacks the nonallylic IPP ligand, a condition that could affect the topology of the active site. For example, recent structural data on a bacterial FPPS, crystallized in the presence of both allylic and nonallylic ligands, indicated that substrate-induced active-site rearrangements result in the C-terminus of the protein interacting with residues that contact IPP.[22]

Unlike the *Dm*FPPS clone, all four lepidopteran FPPSs tested here provided only partial complementation of a yeast FPPS mutation (see Fig. 5). Although this imperfect complementation could be due to the absence of a necessary enhancing factor in the yeast cellular milieu, the possibility that the lepidopteran prenyltransferases form heterodimers under natural conditions should also be considered. It has been generally assumed that FPPSs are active as homodimers, but other prenyltransferases such as plant geranyl diphosphate synthase (GPPS) have

been shown to be active as heterodimers.[61] In the context of this hypothesis, the poor performance of the lepidopteran FPPSs in yeast, and the problems encountered with its recombinant expression in *E. coli*, could be due to heterodimerization with a suboptimal protein partner.

Whether the two types of FPPS cloned here are related to the *B. mori* "FPPS I" and "FPPS II" purified by Koyama et al.[12,13] is unclear at this point. Certainly, the ubiquitous nature of *Bm*FPPS-1 (see Fig. 9), along with the unique features of its active site, which are postulated to be favorable to the formation of ethyl-branched FPP, concur with the authors' description of their "FPPS II", which is reported to be too abundant to be confined to the CA, and which showed a greater ability than "FPPS I" to form the precursors of the ethyl-branched JHs.

CONCLUSIONS

The type-I and type-II lepidopteran FPPS homologs characterized here display important differences in their amino acid sequences, both within and outside their active sites. The structural analysis presented above points to the type-I protein as being the better adapted enzyme for processing ethyl-substituted substrates and products; however, an assessment of each gene's tissue-specific transcription in *B. mori* larvae indicated that the more divergent type-II protein is likely to be a JH-specific FPPS. Whether the type-II FPPSs are the only prenyltransferases involved in lepidopteran JH biosynthesis remains to be determined; of course, there may be additional lepidopteran FPPS types that have not yet been isolated and which could participate in JH biosynthesis. The structural singularities of the type-I proteins and their general distribution suggest that they have other or additional functions as yet unidentified in insects.

ACKNOWLEDGMENTS

The authors thank D. Trudel and S. Patry for technical assistance, F. Couillaud for providing the *A. ipsilon* FPPS cDNA clone, F. Karst for providing the CC25 yeast mutant, J.N. McNeil for giving them access to his *P. unipuncta* rearing, Q. Feng for providing the sequence of an EST corresponding to *Cf*FPPS-1, A. Young and C. Tittiger for providing early access to their coleopteran FPPS sequences, G. Caputo for providing the cell lines, F. Bourque (LiveFood.ca) for providing silkworms, S.-H. Gu and T. Shiotsuki for advice on silkworm CA dissections, and D. Doucet, S.R. Palli, and two anonymous reviewers for critical assessments of earlier versions of the manuscript.

REFERENCES

1. Richard DS, Applebaum SW, Sliter TJ, Baker FC, Schooley DA, Reuter CC, Henrich VC, Gilbert LI. Juvenile hormone bisepoxide biosynthesis *in vitro* by the ring gland of *Drosophila melanogaster*: a putative juvenile hormone in the higher Diptera. Proc Natl Acad Sci USA 1989;86:1421–1425.
2. Schooley DA, Baker FC. Juvenile hormone biosynthesis. In: Kerkut GA, Gilbert LI, editors. Comprehensive insect physiology, biochemistry and pharmacology, Vol. 7. Oxford: Pergamon; 1985. pp 363–389.
3. Schooley DA, Judy KJ, Bergot BJ, Hall MS, Siddall JB. Biosynthesis of juvenile hormones of *Manduca sexta*: labeling pattern from mevalonate, propionate and acetate. Proc Natl Acad Sci USA 1973;70:2921–2925.
4. Koyama T, Ogura K, Seto S. Enzymatic synthesis of bishomofarnesyl pyrophosphate with the insect juvenile hormone skeleton. Chem Lett 1973;401–404.
5. Koyama T, Ogura K, Seto S. Enzymatic synthesis of insect juvenile hormone skeleton. Nippon Kagaku Kaishi 1981;689–696 (in Japanese).
6. Brindle PA, Baker FC, Tsai LW, Reuter CC, Schooley DA. Sources of propionate for the biogenesis of ethyl-branched insect juvenile hormones: role of isoleucine and valine. Proc Natl Acad Sci USA 1987;84:7906–7910.
7. Brindle PA, Baker FC, Tsai LW, Schooley DA. Comparative metabolism of isoleucine by corpora allata of nonlepidopteran insects versus lepidopteran insects, in relation to juvenile hormone biosynthesis. Arch Insect Biochem Physiol 1992;19:1–15.
8. Brindle PA, Schooley DA, Tsai LW, Baker FC. Comparative metabolism of branched-chain amino acids to precursors of juvenile hormone biogenesis in corpora allata of lepidopterous vs nonlepidopterous insects. J Biol Chem 1988;263:10653–10657.
9. Cusson M, Le Page A, McNeil JN, Tobe SS. Rate of isoleucine metabolism in lepidopteran corpora allata: regulation of the proportion of juvenile hormone homologs released. Insect Biochem Mol Biol 1996;26:195–201.
10. Dahm KH, Bhaskaran G, Peter MG, Shirk PD, Seshan KR, Röller H. On the identity of juvenile hormone in insects. In: Gilbert LI, editor. The juvenile hormones. New York: Plenum; 1976. pp 19–47.
11. Peter GM, Shirk PD, Dahm KH, Röller H. On the specificity of juvenile hormone biosynthesis in the male *cecropia* moth. Z Naturforsch 1981;36:579–585.
12. Koyama T, Matsubara M, Ogura K. Isoprenoid enzyme systems of silkworm. I. Partial purification of isopentenyl pyrophosphate isomerase, farnesyl pyrophosphate synthetase, and geranylgeranyl pyrophosphate synthetase. J Biochem 1985;98:449–456.
13. Koyama T, Matsubara M, Ogura K. Isoprenoid enzyme systems of silkworm. II. Formation of the juvenile hormone skeletons by farnesyl pyrophosphate synthase. J Biochem 1985;98:457–463.
14. Sen SE, Ewing GJ, Thurston N. Characterization of lepidopteran prenyltransferase in *Manduca sexta corpora allata*. Arch Insect Biochem Physiol 1996;32:315–332.
15. Sen SE, Ewing GJ. Natural and unnatural terpenoid precursors of insect juvenile hormone. J Org Chem 1997;62:3529–3536.
16. Kellogg BA, Poulter CD. Chain elongation in the isoprenoid biosynthetic pathway. Curr Opin Chem Biol 1997;1:570–578.
17. Koyama T, Ogura K. Isopentenyl diphosphate isomerase and prenyltransferases. In: Barton D, Nakanishi K, editors. Comprehensive natural product chemistry, Vol. 2. Oxford: Elsevier Science; 1999. pp 69–96.
18. Wang K, Ohnuma S. Chain-length determination mechanism of isoprenyl diphosphate synthases and implications for molecular evolution. Trends Biochem Sci 1999;24:445–451.
19. Liang PH, Ko TP, Wang AH. Structure, mechanism and function of prenyltransferases. Eur J Biochem 2002;269:3339–3354.
20. Tarshis LC, Yan M, Poulter CD, Sacchettini JC. Crystal structure of recombinant farnesyl diphosphate synthase at 2.6-Å resolution. Biochemistry 1994;13:10871–10877.
21. Tarshis LC, Proteau PJ, Kellogg BA, Sacchettini JC, Poulter CD. Regulation of product chain length by isoprenyl diphosphate synthases. Proc Natl Acad Sci USA 1996;93:15018–15023.
22. Hosfield DJ, Zhang Y, Dougan DR, Broun A, Tari LW, Swanson RV, Finn J. Structural basis for bisphosphonate-mediated inhibition of isoprenoid biosynthesis. J Biol Chem 2004;279:8526–8529.
23. Mao J, Gao YG, Odeh S, Robinson H, Montalvetti A, Docampo R, Oldfield E. Crystallization and preliminary X-ray diffraction study of the farnesyl diphosphate synthase from *Trypanosoma brucei*. Acta Crystallogr Biol D Crystallogr 2004;60:1863–1866.
24. Cusson M, Palli SR. Can juvenile hormone research help rejuvenate integrated pest management? Can Entomol 2000;132:263–280.
25. Castillo-Gracia M, Couillaud F. Molecular cloning and tissue expression of an insect farnesyl diphosphate synthase. Eur J Biochem 1999;262:365–370.

26. Kikuchi K, Hirai M, Shiotsuki T. Molecular cloning and tissue distribution of farnesyl pyrophosphate synthase from the silkworm *Bombyx mori*. J Insect Biotechnol Sericology 2001;70:167–172.
27. Cusson M, Delisle J. Effect of mating on plasma juvenile hormone esterase activity in females of *Choristoneura fumiferana* and *C. rosaceana*. Arch Insect Biochem Physiol 1996;32:585–599.
28. Francis F, Lognay G, Wathelet JP, Haubruge E. Effects of allelochemicals from first (Brassicaceae) and second (*Myzus persicae* and *Brevicoryne brassicae*) trophic levels on *Adalia bipunctata*. J Chem Ecol 2001;27:243–256.
29. Sohi SS, Lalouette W, Macdonald JA, Gringorten JL, Budau CB. Establishment of continuous midgut cell lines of spruce budworm (Lepidoptera: Tortricidae). In Vitro Cell Dev Biol 1993; 29A:56A.
30. Bilimoria SL, Sohi SS. Development of an attached strain from a continuous insect cell line. In Vitro 1977;13:461–466.
31. Béliveau C, Levasseur A, Stoltz D, Cusson M. Three related TrIV genes: comparative sequence analysis and expression in host larvae and CF-124T cells. J Insect Physiol 2003;49:501–511.
32. Chambon C, Ladeveze V, Oulmouden A, Servouse M, Karst F. Isolation and properties of yeast mutants affected in farnesyl diphosphate synthetase. Curr Genet 1990;18:41–46.
33. Minet M, Dufour ME, Lacroute F. Complementation of *Saccharomyces cerevisiae* auxotrophic mutants by *Arabidopsis thaliana* cDNAs. Plant J 1992;2:417–422.
34. Meilhoc E, Masson JM, Teissie J. High efficiency transformation of intact yeast cells by electric field pulses. Biotechnology 1990; 8:223–227.
35. Thompson JD, Gibson TJ, Plewniak F, Jeanmougin F, Higgins DG. The ClustalX windows interface: flexible strategies for multiple sequence alignment aided by quality analysis tools. Nucleic Acids Res 1997;24:4876–4882.
36. Swofford DL. PAUP* 4.0b10: phylogenetic analysis using parsimony (*and other methods), Version 4.0b10, Sinauer Associates, Sunderland, MA.
37. Brooks BR, Bruccoleri RE, Olafson BD, States DJ, Swaminathan S, Karplus M. Charmm—a program for macromolecular energy minimization and dynamics calculations. J Comput Chem 1983;4:187–217.
38. Laskowski RA, MacArthur MW, Moss DS, Thornton JM. PROCHECK: a program to check the stereochemical quality of protein structures. J Appl Cryst 1993;26:283–291.
39. Guex N, Peitsch MC. SWISS-MODEL and the Swiss-PdbViewer: an environment for comparative protein modeling. Electrophoresis 1997;18:2714–2723.
40. MacKerell AD, Jr, Bashford D, Bellott M, Dunbrack RL, Jr, Evanseck JD, Field MJ, Fischer S, Gao J, Guo H, Ha S, Joseph-McCarthy D, Kuchnir L, Kuczera K, Lau FTK, Mattos C, Michnick S, Ngo T, Nguyen DT, Prodhom B, Reiher WE III, Roux B, Schlenkrich M, Smith JC, Stote R, Straub J, Watanabe M, Wiórkiewicz-Kuczera J, Yin D, Karplus M. All-atom empirical potential for molecular modeling and dynamics studies of proteins. J Phys Chem B 1998;102:3586–3616.
41. Shinoda T, Itoyama K. Juvenile hormone acid methyltransferase: a key regulatory enzyme for insect metamorphosis. Proc Natl Acad Sci USA 2003;100:11986–11991.
42. Rutledge RG Sigmoidal curve-fitting redefines quantitative real-time PCR with the prospective of developing automated high-throughput applications. Nucleic Acids Res 2004;32:e178.
43. Gouet P, Courcelle E, Stuart DI, Metoz F. ESPript: multiple sequence alignments in PostScript. Bioinformatics 1999;15:305–308.
44. von Heijne G. Cleavage-site motifs in protein targeting sequences. Genet Eng 1992;14:1–11.
45. Koyama T, Obata S, Osabe M, Takeshita A, Yokoyama K, Uchida M, Nishino T, Ogura K. Thermostable farnesyl diphosphate synthase of *Bacillus stearothermophilus*: molecular cloning, sequence determination, overproduction, and purification. J Biochem Tokyo 1993;113:355–363.
46. Bellés X, Martín D, Piulachs M-D. The mevalonate pathway and the synthesis of juvenile hormone in insects. Annu Rev Entomol 2005;50:181–199.
47. Nielsen ES. Phylogeny of major lepidopteran groups. In: Fernholm B, Bremer K, Jörnvall H, editors. The hierarchy of life. Amsterdam: Elsevier Science; 1989. pp 281–294.
48. Sen SE, Sperry AE. Partial purification of a farnesyl diphosphate synthase from whole-body *Manduca sexta*. Insect Biochem Mol Biol 2002;32:889–899.
49. Joly A, Edwards PA. Effect of site-directed mutagenesis of conserved aspartate and arginine residues upon farnesyl diphosphate synthase activity. J Biol Chem 1993;268:26983–26989.
50. Song L, Poulter CD. Yeast farnesyl-diphosphate synthase: site-directed mutagenesis of residues in highly conserved prenyltransferase domains I and II. Proc Natl Acad Sci USA 1994;91: 3044–3048.
51. Ohnuma S, Hirooka K, Hemmi H, Ishida C, Ohto C, Nishino T. Conversion of product specificity of archaebacterial geranylgeranyl-diphosphate synthase. Identification of essential amino acid residues for chain length determination of prenyltransferase reaction. J Biol Chem 1996;271:18831–18837.
52. Ohnuma S, Narita K, Nakazawa T, Ishida C, Takeuchi Y, Ohto C, Nishino T. A role of the amino acid residue located on the fifth position before the first aspartate-rich motif of farnesyl diphosphate synthase on determination of the final product. J Biol Chem 1996;271:30748–30754.
53. Narita K, Ohnuma S, Nishino T. Protein design of geranyl diphosphate synthase. Structural features that define the product specificities of prenyltransferases. J Biochem Tokyo 1999; 126:566–571.
54. Fernandez SMS, Kellogg BA, Poulter CD. Farnesyl diphosphate synthase. Altering the catalytic site to select for geranyl diphosphate activity. Biochemistry 2000;39:15316–15321.
55. Ohnuma S, Hirooka K, Tsuruoka N, Yano M, Ohto C, Nakane H, Nishino T. A pathway where polyprenyl diphosphate elongates in prenyltransferase. Insight into a common mechanism of chain length determination of prenyltransferases. J Biol Chem 1998;273: 26705–26713.
56. Hemmi H, Noike M, Nakayama T, Nishino T. An alternative mechanism of product chain-length determination in type III geranylgeranyl diphosphate synthase. Eur J Biochem 2003; 270:2186–2194.
57. Kawasaki T, Hamano Y, Kuzuyama T, Itoh N, Seto H, Dairi T. Interconversion of the product specificity of type I eubacterial farnesyl diphosphate synthase and geranylgeranyl diphosphate synthase through one amino acid substitution. J Biochem Tokyo 2003;133:83–91.
58. Cusson M, McNeil JN, Tobe SS. In vitro biosynthesis of juvenile hormone by corpora allata of *Pseudaletia unipuncta* virgin females as a function of age, environmental conditions, calling behaviour and ovarian development J Insect Physiol 1990;36: 139–146.
59. Horsman GP, Liu AM, Henke E, Bornscheuer UT, Kazlauskas RJ. Mutations in distant residues moderately increase the enantioselectivity of *Pseudomonas fluorescens* esterase towards methyl 3bromo-2-methylpropanoate and ethyl 3phenylbutyrate. Chemistry 2003;9:1933–1939.
60. Zhang J, Dean AM, Brunet F, Long M. Evolving protein functional diversity in new genes of *Drosophila*. Proc Natl Acad Sci USA 2004;101:16246–16250.
61. Burke CC, Wildung MR, Croteau R. Geranyl diphosphate synthase: cloning, expression, and characterization of this prenyltransferase as a heterodimer. Proc Natl Acad Sci USA 1999;96: 13062–13067.